Analysis of a commercial small unmanned airborne system (sUAS) in support of the Radiometric Calibration Test Site (RadCaTS) at Railroad Valley

Jeffrey S. Czapla-Myers, Nikolaus J. Anderson

Jeffrey S. Czapla-Myers, Nikolaus J. Anderson, "Analysis of a commercial small unmanned airborne system (sUAS) in support of the Radiometric Calibration Test Site (RadCaTS) at Railroad Valley," Proc. SPIE 10402, Earth Observing Systems XXII, 104020K (5 September 2017); doi: 10.1117/12.2274478

SPIE.

Event: SPIE Optical Engineering + Applications, 2017, San Diego, California, United States

Analysis of a commercial small unmanned airborne system (sUAS) in support of the Radiometric Calibration Test Site (RadCaTS) at Railroad Valley

Jeffrey S. Czapla-Myers* and Nikolaus J. Anderson
Remote Sensing Group, College of Optical Sciences, University of Arizona,
1630 E University Blvd, Tucson, AZ, USA 85721–0094

ABSTRACT

The Radiometric Calibration Test Site (RadCaTS) is an automated facility developed by the Remote Sensing Group (RSG) at the University of Arizona to provide radiometric calibration data for airborne and satellite sensors. RadCaTS uses stationary ground-viewing radiometers (GVRs) to spatially sample the surface reflectance of the site. The number and location of the GVRs is based on previous spatial, spectral, and temporal analyses of Railroad Valley. With the increase in high-resolution satellite sensors, there is renewed interest in examining the spatial uniformity the 1-km^2 RadCaTS area at scales smaller than a typical 30-m sensor. RadCaTS is one of the four instrumented sites currently in the CEOS WGCV Radiometric Calibration Network (RadCalNet), which aims to harmonize the post-launch radiometric calibration of satellite sensors through the use of a global network of automated calibration sites. A better understanding of the RadCaTS spatial uniformity as a function of pixel size will also benefit the RadCalNet work. RSG has recently acquired a commercially-available small unmanned airborne system (sUAS) system, with which preliminary spatial homogeneity measurements of the 1-km^2 RadCaTS area were made. This work describes an initial assessment of the airborne platform and integrated camera for spatial studies of RadCaTS using data that were collected in 2016 and 2017.

Keywords: sUAS, UAV, camera, calibration, radiometry, RadCaTS

1. INTRODUCTION

The Remote Sensing Group of the College of Optical Sciences at the University of Arizona has been directly involved in the preflight and post-launch radiometric calibration of Earth-observing sensors for over 30 years.[1-14] In the past, various in situ measurement techniques were used to determine the top-of-atmosphere (TOA) spectral radiance for sensors under test,[1,6] but the reflectance-based approach has been the main field technique for the past 15 years.[7] It requires ground personnel to make measurements of the surface reflectance and atmosphere during a given time of interest (e.g. satellite or aircraft overpass). The results of the surface reflectance and atmospheric characterization are used in a radiative transfer code to determine the TOA spectral radiance. Currently, RSG uses the MODerate resolution atmospheric TRANsmission (MODTRAN) radiative transfer code.

RSG has used various ground test sites over the years, such as White Sands Missile Range, New Mexico, Ivanpah Playa, California, Red Lake, Arizona, Alkali Lake, Nevada, and Railroad Valley, Nevada. In recent years, Railroad Valley has become the primary site, with Ivanpah Playa and Alkali Lake acting as secondary test sites. The favorable characteristics that make Railroad Valley a sound vicarious calibration test site are its large size (~15×15 km), high altitude (1435 m), arid conditions, relatively high surface bidirectional reflectance factor (BRF)[15], and remote location. It was originally chosen as a new test site in the late 1990s in response to upcoming work with Landsat-7 Enhanced Thematic Mapper Plus (ETM+) and the Moderate Resolution Imaging Spectroradiometer (MODIS) onboard the Terra platform.[16,17] The 1-km pixel of MODIS requires a much larger homogenous area to ensure that there are minimal adjacency effects. There are three areas at Railroad Valley used for surface reflectance measurements, and their use depends on the configuration of the sensor being calibrated. Fig. 1 shows the three areas: pushbroom, whiskbroom, and large ground-instantaneous field of view (GIFOV). The pushbroom area is 80×300 m, and is used for sensors such as the Advanced Spaceborne Thermal Emission and Reflection radiometer (ASTER) and the RapidEye constellation of satellites.[18] The whiskbroom area is 120×480 m, and is used for Landsat 5 TM and Landsat-7 ETM+. Finally, the large GIFOV site is 1 km^2 and is used for sensors such as MODIS, the Suomi NPP Visible Infrared Imaging Radiometer Suite (VIIRS), and most recently the Advanced Baseline Imager (ABI) onboard the Geostationary Operational Environmental Satellite 16 (GOES-16).

*jscm@optics.arizona.edu; phone +1.520.621.4242; wp.optics.arizona.edu/rsg

Earth Observing Systems XXII, edited by James J. Butler, Xiaoxiong (Jack) Xiong, Xingfa Gu, Proc. of SPIE Vol. 10402, 104020K · © 2017 SPIE · CCC code: 0277-786X/17/$18 · doi: 10.1117/12.2274478

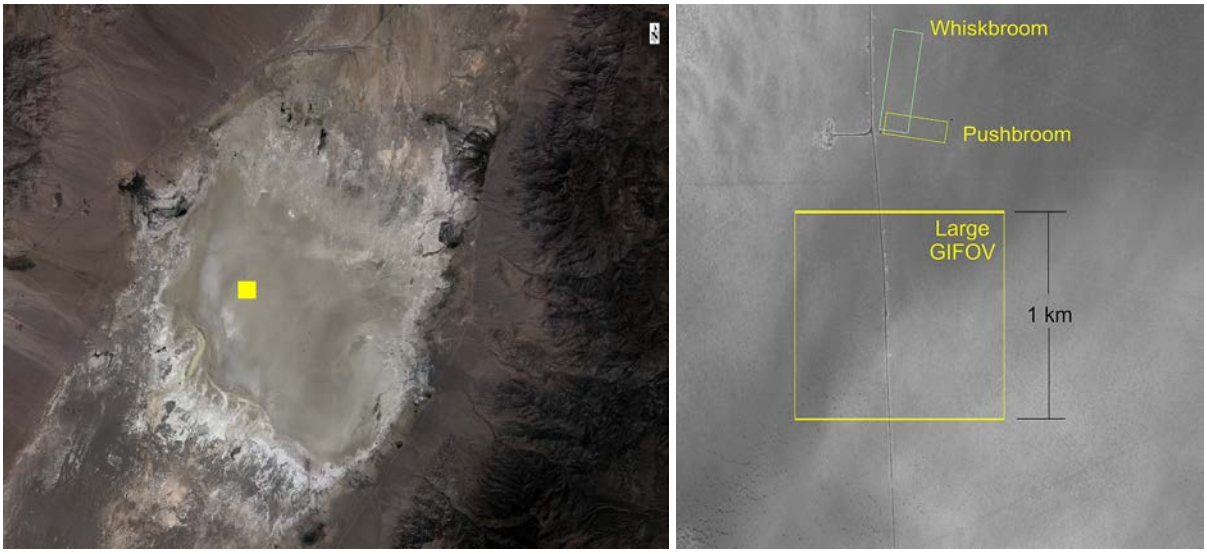

Fig. 1. Railroad Valley, Nevada (left), and the three areas used with the reflectance-based approach (right). The pushbroom area is 80×300 m, and the whiskbroom area is 120×300 m. The line running north-south in the right image is a dirt road used for access to the site.

RSG research efforts over the past 15 years have included the automation of ground-based vicarious calibration, similar to the inland water bodies that are used for the midwave and thermal infrared.[19-21] Railroad Valley was chosen as the site since it would be used with large-footprint sensors such as MODIS. One of the first tasks was to identify instrumentation that could be used to measure the surface BRF and atmosphere in place of the instruments that RSG typically bring to the site during every field campaign. RSG had already been operating an Aerosol Robotic Network (AERONET) Cimel CE318 sun photometer, so it was determined that this would continue to be used for the automated site. The next challenge was to develop a radiometer that was suitable for the permanent deployment at a remote location, and was able to collect data throughout the year. Early prototype ground-viewing radiometers (GVRs) were used to measure the surface BRF in three visible and near-infrared (VNIR) channels using light-emitting diodes (LEDs) as detectors.[22] The development of prototype GVRs was conducted in tandem with studies of Railroad Valley to determine the number and placement of GVRs that was required to spatially sample the site with a similar accuracy as the reflectance-based approach.[23,24] It was determined that at least four GVRs were required to sample the 1-km^2 area of Railroad Valley to have a BRF uncertainty of ±2%.

The prototype GVRs were successfully used to create a processing scheme that combined the surface BRF measurements and the Cimel data to be used as input into MODTRAN. Early work showed reasonable agreement with satellite observations, but the prototype radiometers were clearly becoming the largest source of uncertainty. They were each calibrated and characterized in RSG's laboratory before deployment, and this included their spectral, spatial, and radiometric characteristics. The spectral characteristics as a function of temperature were not characterized, so it was determined that upgraded GVRs were needed to eliminate effects due to the temperatures at Railroad Valley (–20°C to +40°C throughout the year). In 2010, work began on the new design for GVRs, and they were deployed in 2011–2012. As with the prototype GVRs, the new models were calibrated and characterized in the laboratory before deployment to Railroad Valley.[25,26]

The automated site at Railroad Valley has become known as the Radiometric Calibration Test Site (RadCaTS), and it currently has five GVRs located throughout the 1-km^2 area that defines RadCaTS. Four GVRs are in a nadir-viewing configuration, while one is in a viewing configuration similar to GOES-16 for work with ABI (Fig. 2). Atmospheric measurements continue to be made using a Cimel CE318-T solar and lunar photometer, and there is a meteorological station to make ancillary measurements such as temperature, pressure, wind speed and direction, and precipitation. The GVRs are deployed in locations that are a compromise between appropriate spatial sampling and easy accessibility from the road that runs north-south through the site. During the prototyping phase of GVR development, the LED-based instruments had to be routinely radiometrically calibrated using the solar-radiation-based calibration (SRBC) method,[27] which requires that equipment including a Spectralon reference panel be carried to each radiometer during the calibration

Fig. 2. One of the GVRs at RadCaTS (left), and a Cimel CE318-T (left) solar and lunar photometer.

process. Because of this, the GVR furthest from the road is located ~165 m from the road. Periodic radiometric calibration measurements of the GVRs are now completed using the Calibration Test Site SI-Traceable Transfer Radiometer (CaTSSITTR), which is a portable laboratory-grade transfer radiometer developed at RSG to monitor the on-site instrumentation used to make surface BRF measurements.[28] In 2015, the RSG mobile laboratory was converted to a satellite uplink base station, which is used as WiFi hub for the wireless data loggers at each GVR. Data are sent from each GVR and the meteorological station to the mobile base station, and then the data are uploaded to the University of Arizona once per day via a satellite uplink. Fig. 3 shows the current layout of RadCaTS at Railroad Valley.

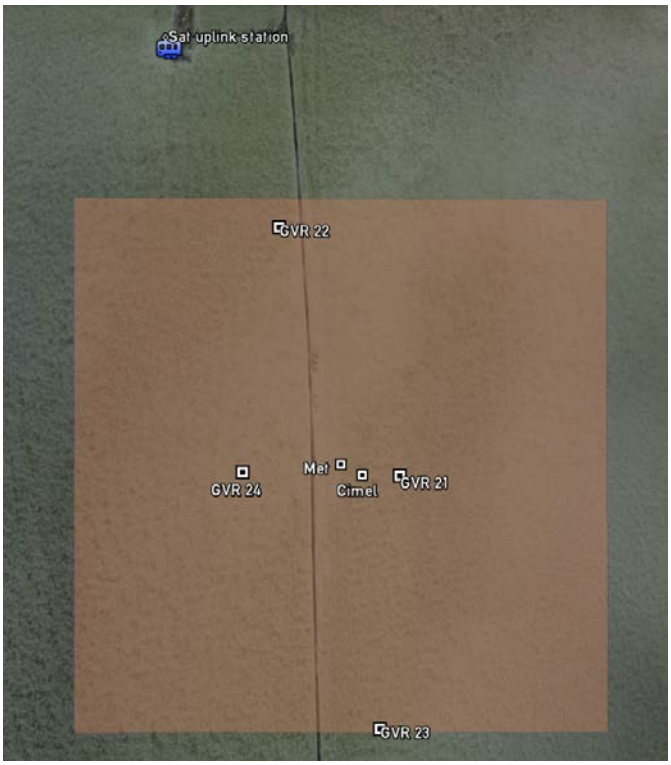

Fig. 3. The current layout of RadCaTS. The brown box is the 1×1-km region of interest. GVR 25 is located next to GVR 23.

RadCaTS is one of four automated test sites that make up the Radiometric Calibration Network (RadCalNet), which is organized by the Committee on Earth Observation Satellites (CEOS) Working Group on Calibration and Validation

(WGCV). The goal of RadCalNet is to coordinate the efforts of international space agencies to facilitate harmonization and interoperability of satellite imaging sensors with SI traceability. It has been in a prototyping stage since 2014, is currently undergoing beta testing, and will go live to registered users beginning in late 2017 (www.radcalnet.org). One of the requirements of RadCalNet is a well-documented uncertainty chain, which includes the calibration of the instruments used at each site, and also the site itself.

RSG has acquired a sUAS in an effort to measure the spatial homogeneity of the 1-km^2 RadCaTS area, which would be nearly impossible with the typical portable spectroradiometer that is used to measure the surface BRF. In order to create science-level data from measurements made using the integrated camera system on the sUAS, laboratory measurements were made in order to understand the radiometric responsivity of the camera, and also the relative spectral response (RSR). This paper describes the laboratory calibration, and also presents results of preliminary field measurements.

2. METHODOLOGY

The sUAS used in this work is the Da-Jiang Innovations Science and Technology Co. Ltd (DJI) Phantom 3 Professional, hereby referred to as the DJI P3. It is a commercially-available quadcopter with an integrated, gimbal-mounted, 12.4-megapixel camera, which operates at a fixed f/2.8 f stop, 94° full field of view, and fixed focus at infinity (Fig. 4). The integrated camera uses a Sony Exmor 1/2.3-inch complementary metal oxide semiconductor (CMOS) sensor that has an ISO range of 100–1600, shutter speed of 8–1/8000 s, 12-bit radiometric resolution, and a maximum spatial dimension of 3000×4000 pixels. The images produced by the camera are saved in JPEG and/or Digital Negative (DNG) format. The challenge when working with commercial systems is to understand the image processing steps that convert the raw camera data to a viewable image. This work uses uncompressed DNG images, which allow access to the 12-bit raw data directly from the camera and also the ancillary information found in the Exchangeable Image File (EXIF) meta information that is included with each image. The DNG images are processed using the Matrix Laboratory (MATLAB) software package.[29]

Fig. 4. DJI Phantom 3 Professional at RadCaTS.

3. DATA

The preliminary analysis of the DJI P3 includes laboratory measurements of the camera sensor to determine the absolute radiometric calibration, linearity, and RSR of the red, green and blue (RGB) channels. Measurements in the field were also used to assess the preliminary validation of the image processing technique. The laboratory measurements were made in RSG's radiometric calibration facility, which includes a 1-m spherical integrating source (SIS) to provide the absolute radiometric calibration and linearity of the camera, and an Optronic OL750 double monochromator to measure the RSR of the RGB channels. Field measurements were made at RadCaTS, and also at the University of Arizona.

The radiometric calibration and linearity of the DJI P3 camera were conducted using the 1-m SIS as an output source. The DJI P3 was placed close enough to the SIS so as to view the entire exit port (Fig. 5). An absolutely-calibrated portable hyperspectral spectroradiometer viewed the SIS simultaneously in order to measure the output spectral radiance from 400–2500 nm. The DJI P3 camera was used in manual mode, where the user can set various settings for the camera, such as the white balance, shutter speed, and ISO. There is a very large combination of settings that are possible, so it was important to choose values that were going to be typically used at RadCaTS, otherwise the tests would become too cumbersome. The white balance was manually set to 5500 K, and the ISO was set to 100. This left the shutter speed, which was varied from 1/8000 s to saturation exposure. The linearity of the camera sensor was measured in tandem with the absolute radiometric calibration by first starting with the SIS illuminated by ten 150-W lamps. Then, after going through all of the possible shutter speeds, the SIS lamps were turned off. The complete sequence of lamps was: 10, 8, 6, 4, 2, and 1.

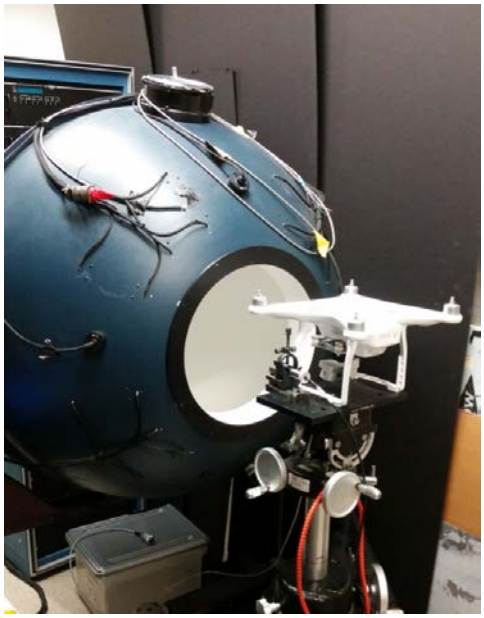

Fig. 5. DJI P3 and portable spectroradiometer foreoptic in front of the 1-m SIS, which is not illuminated in this image.

The RSR was measured by placing the DJI P3 at the exit port of the Optronic OL750 double monochromator. The same values for white balance and ISO in the radiometric calibration measurements were used, and images were taken with various shutter speeds to determine if there were any possible effects. The slits on the Optronic were chosen so that the spectral bandwidth was ~2.5 nm, and measurements were made from 400–800 nm, in 10-nm increments. The measurement was performed multiple times over the span of a few days to assess repeatability.

Field validation data were collected at RadCaTS in March 2017, and also at the University of Arizona in April 2017. At RadCaTS, imagery was collected in a nadir-viewing configuration with the DJI P3 at various altitudes, and images included a Spectralon reference panel and/or a GVR. The BRF of the Spectralon panel is measured annually in RSG's laboratory, so its BRF is known as a function of angle and wavelength. It is then used as the reference to determine the surface BRF using a ratio of the ground measurements to those of the panel. This is effectively how the surface BRF is measured using the reflectance-based approach.[7] In the case of imagery that contains a GVR, the band-averaged spectral radiance can be compared, assuming that the DJI P3 altitude is not very high. An example of imagery taken at RadCaTS, which includes both a Spectralon panel and a GVR, is shown in Fig. 6.

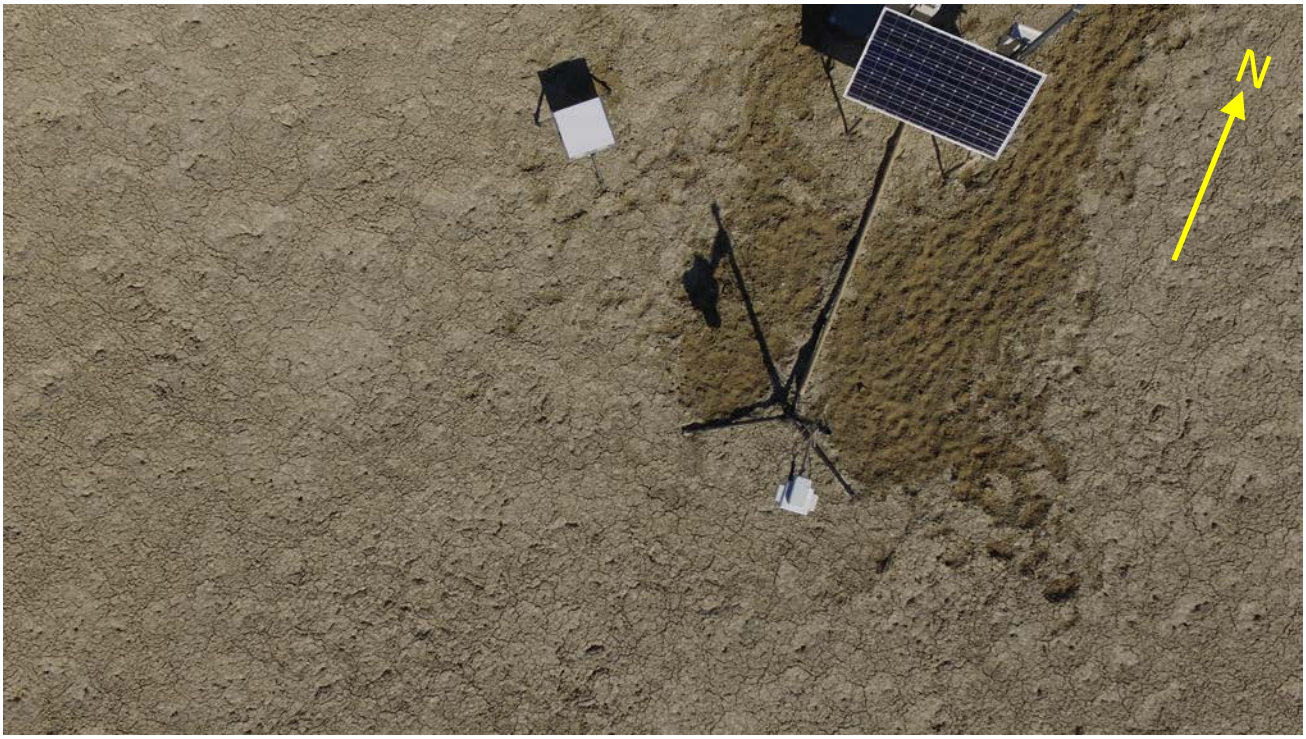

Fig. 6. An 8-bit JPG version of a RAW image taken with the DJI P3 at RadCaTS. A Spectralon panel is located center-top, and the GVR in Fig. 2 is located near the center of the image. The dark rectangle near the top is a solar panel, which is used to charge the GVR and data logger batteries. The dimensions of the Spectralon panel are 46×46 cm.

4. RESULTS

The absolute radiometric calibration and linearity results depend on the RSR measurements, so they are presented first. The normalized RSR for each of the RGB channels is shown in Fig. 7. The camera settings were typical of those used in the field: 100 ISO, 1/3200-s shutter speed, and a white balance of 5500 K. Repeated measurements yielded similar results.

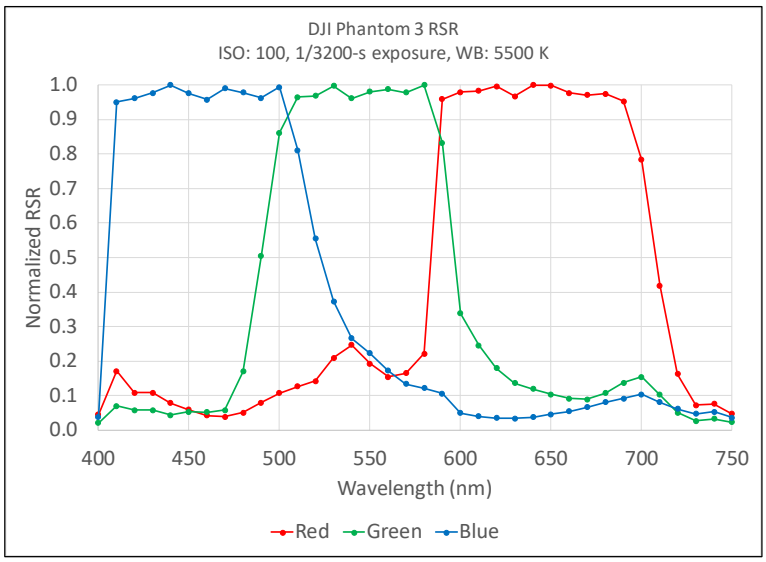

Fig. 7. Results for the RSR measurements of the DJI P3 camera.

Once the RSR of the DJI P3 camera was determined, the absolute radiometric calibration was determined for the DJI P3 camera by comparing the digital numbers (DNs) of the camera to the absolutely calibrated SIS data as measured by the portable spectroradiometer. For the typical field settings of 100 ISO, 1/3200-s shutter speed, and a white balance of 5500 K, the initial results of the relation between camera DNs and the band-averaged spectral radiance is shown in Fig. 8 for the red, green, and blue channels. The red and green channels appear to have an exponential relationship between the DNs and band-averaged spectral radiance, but there is noise in the results for blue channel that still need to be understood. Additional laboratory measurements will be made in the future to further investigate this relationship.

Fig. 8. Absolute calibration results from the SIS measurements with the DJI P3 camera.

A preliminary spatial analysis of the DJI P3 image in Fig. 6 consisted of comparing the surface BRF for a region of interest (ROI) near the GVR to the BRF determined using the GVR. The surface BRF determined using the DJI P3 was calculated by using the reflectance-based methodology, where the surface BRF is determined using the ratio of the DNs over the ground to those over the panel, multiplied by the known BRF of the panel. The ROI of the panel and the ground are shown

in Fig. 9 which is a magnified version of Fig. 6 with the ROIs included. The size of the ROI next to the GVR is ~30 cm in diameter, which is similar to the spot size on the ground for a GVR. Its location was chosen in an attempt to match the area on the ground measured by the GVR.

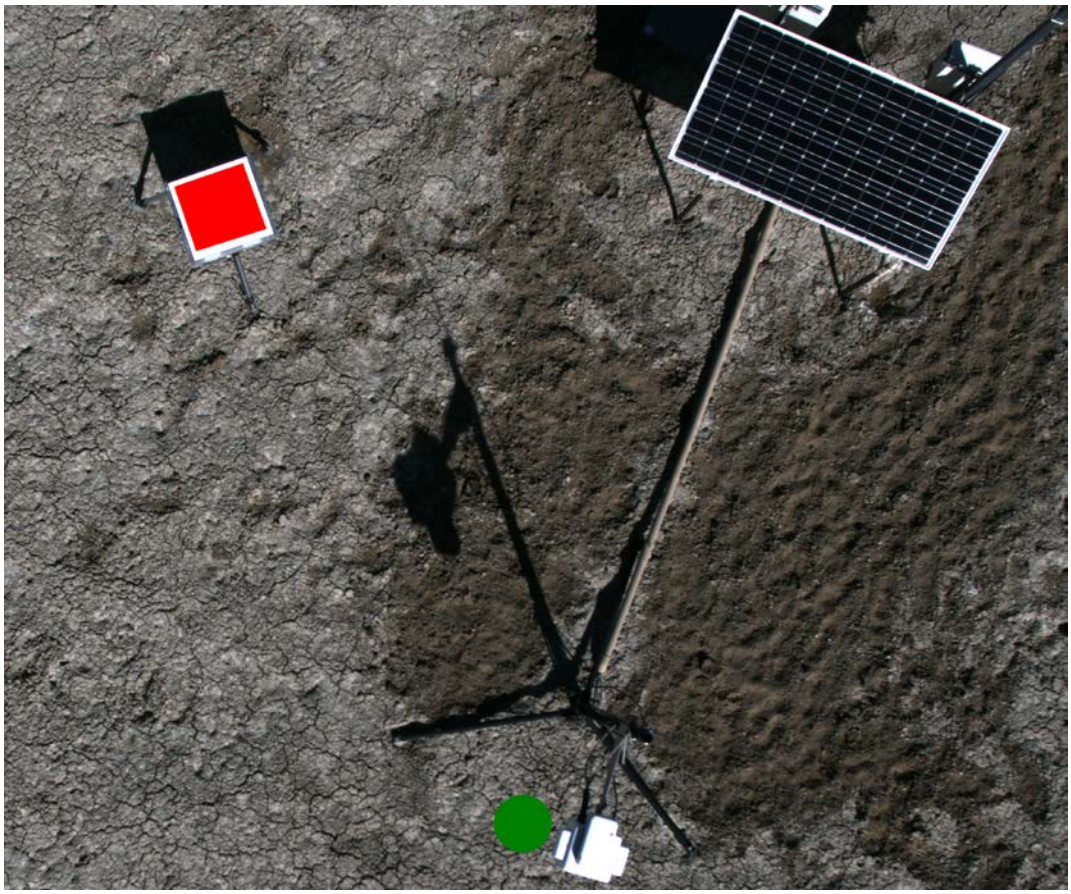

Fig. 9. The regions of interest (ROIs) are the Spectralon reference panel (red) and the ground under the GVR (green), which are used in the reflectance-based approach to determine the surface BRF of the green ROI.

The results of the comparison between the DJI P3 and the GVR are shown in Fig. 10, where only the three channels of the GVR close to those of the DJI P3 camera are shown. The absolute difference between the two systems is larger than one would want, but the sky conditions were less than ideal for such a comparison. For example, the Angstrom exponent, which describes the aerosol optical depth as a function of wavelength, was 0.55. This measurement would be rejected in the current processing scheme for RadCaTS and RadCalNet, where a 'good day' is considered to have Angstrom exponent values ranging from 0.9–1.5. The difference between the retrieved BRF values from the GVR and sUAS is therefore considered acceptable for the preliminary measurements presented here.

5. CONCLUSIONS

RSG has incorporated a commercial sUAS to help characterize the spatial homogeneity of RadCaTS. The main advantage to using an sUAS is the ability to measure a large or small area over a reasonably short period of time. Even with the restricted spectral coverage offered by the integrated camera system, the results from these measurements will assist the group in characterizing the uncertainty of the RadCaTS data processing, which can be affected by spatial sampling issues created by the limited number of GVRs that are used to spatially sample the 1-km^2 site. The initial laboratory measurements using RAW imagery revealed that the linearity table, which is available in many professional-grade digital cameras, is not available in the EXIF data of the DJI P3. This is observed in the nonlinear results obtained during the absolute radiometric calibration measurements, which means that there are proprietary image processing algorithms in use that are not available to the end user. RSG will perform more laboratory calibration measurements to further understand the nonlinear behavior

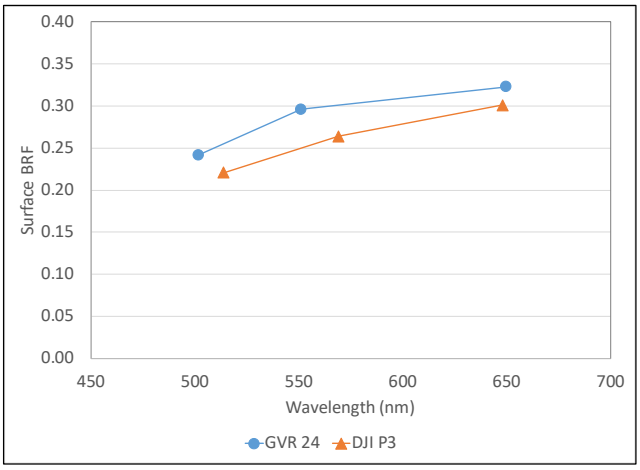

Fig. 10. Results of a surface BRF comparison between a GVR and the DJI P3 sUAS.

of the sensor when used with various ISO, shutter speed, and white balance settings. One potential issue that was not addressed is the effect of temperature on the responsivity of the camera. It is currently beyond the scope of this work and may or may not be addressed in the future. The preliminary measurements of surface BRF using the sUAS were considered successful, even though the weather conditions were less than favorable. Future field work will include similar measurements to further assess the capabilities of the sUAS at a variety of spatial sampling scales.

ACKNOWLEDGEMENTS

The authors would like to thank the Bureau of Land Management (BLM) Tonopah, Nevada, office for their assistance and permission in using Railroad Valley, and also AERONET for processing the Cimel data. The authors would also like to acknowledge NASA for funding this work.

REFERENCES

[1] P. N. Slater, S. F. Biggar, R. G. Holm, R. D. Jackson, Y. Mao, M. S. Moran, J. M. Palmer, and B. Yuan, “Reflectance- and radiance-based methods for the in-flight absolute calibration of multispectral sensors,” Remote Sensing of Environment, 22(1), 11-37 (1987).

[2] S. F. Biggar, M. Dinguirard, D. I. Gellman, P. Henry, R. D. Jackson, M. S. Moran, and P. N. Slater, "Radiometric calibration of SPOT 2 HRV - A comparison of three methods." Proc. SPIE 1493, 155-162 (1991).

[3] S. F. Biggar, P. N. Slater, K. J. Thome, A. W. Holmes, and R. A. Barnes, "Preflight solar-based calibration of SeaWiFS." Proc. SPIE 1939, 233-242 (1993).

[4] K. J. Thome, D. I. Gellman, R. J. Parada, S. F. Biggar, P. N. Slater, and M. S. Moran, "In-flight radiometric calibration of Landsat-5 Thematic Mapper from 1984 to present." Proc. SPIE 1938, 126-130 (1993).

[5] P. N. Slater, S. F. Biggar, K. J. Thome, D. I. Gellman, and P. R. Spyak, “Vicarious Radiometric Calibrations of EOS Sensors,” Journal of Atmospheric and Oceanic Technology, 13(2), 349-359 (1996).

[6] K. J. Thome, B. G. Crowther, and S. F. Biggar, “Reflectance- and Irradiance-based Calibration of Landsat 5 Thematic Mapper,” Canadian Journal of Remote Sensing, 23(4), 309-317 (1997).

[7] K. J. Thome, “Absolute radiometric calibration of Landsat 7 ETM+ using the reflectance-based method,” Remote Sensing Environment, 78, 27-38 (2001).

[8] P. N. Slater, S. F. Biggar, J. M. Palmer, and K. J. Thome, “Unified approach to absolute radiometric calibration in the solar-reflective range,” Remote Sensing of Environment, 77(3), 293-303 (2001).

[9] K. J. Thome, J. S. Czapla-Myers, and S. F. Biggar, "Vicarious calibration of Aqua and Terra MODIS." Proc. SPIE 5151, 395-405 (2003).

[10] K. J. Thome, S. F. Biggar, and H. J. Choi, "Vicarious calibration of Terra ASTER, MISR, and MODIS." Proc. SPIE 5542, 290-299 (2004).
[11] K. J. Thome, S. F. Biggar, N. Anderson, J. Czapla-Myers, R. B. Lockwood, S. J. Miller, T. W. Cooley, T. G. Chrien, S. J. Schiller, J. F. Silny, and M. A. Glennon, "Preflight and Vicarious Calibration of ARTEMIS." Proc. IEEE Geoscience and Remote Sensing Symposium (IGARSS) 1, I-249 - I-252 (2008).
[12] J. S. Czapla-Myers, K. Thome, S. Biggar, and N. J. Anderson, "The absolute radiometric calibration of Terra imaging sensors: MODIS, MISR, and ASTER." Proc. SPIE 9218(2014).
[13] J. Czapla-Myers, J. McCorkel, N. Anderson, K. Thome, S. Biggar, D. Helder, D. Aaron, L. Leigh, and N. Mishra, "The Ground-Based Absolute Radiometric Calibration of Landsat 8 OLI," Remote Sensing, 7(1), 600-626 (2015).
[14] J. Czapla-Myers, L. Ong, K. Thome, and J. McCorkel, "Validation of EO-1 Hyperion and Advanced Land Imager Using the Radiometric Calibration Test Site at Railroad Valley, Nevada," Selected Topics in Applied Earth Observations and Remote Sensing, IEEE Journal of, PP(99), 1-11 (2015).
[15] G. Schaepman-Strub, M. E. Schaepman, T. H. Painter, S. Dangel, and J. V. Martonchik, "Reflectance quantities in optical remote sensing--definitions and case studies," Remote Sensing of Environment, 103(1), 27-42 (2006).
[16] K. P. Scott, K. J. Thome, and M. R. Brownlee, "Evaluation of the Railroad Valley Playa for use in vicarious calibration." Proc. SPIE 2818, 158-166 (1996).
[17] K. Thome, N. Smith, and K. Scott, "Vicarious calibration of MODIS using Railroad Valley Playa." Proc. International Geoscience and Remote Sensing Symposium 2001 (IGARSS) 3, 1209-1211 (2001).
[18] D. Naughton, A. Brunn, J. Czapla-Myers, S. Douglass, M. Thiele, H. Weichelt, and M. Oxfort, "Absolute radiometric calibration of the RapidEye multispectral imager using the reflectance-based vicarious calibration method," Journal of Applied Remote Sensing, 5(1), 053544-053544-23 (2011).
[19] S. J. Hook, W. B. Clodius, L. Balick, R. E. Alley, A. Abtahi, R. C. Richards, and S. G. Schladow, "In-Flight Validation of Mid- and Thermal Infrared Data From the Multispectral Thermal Imager (MTI) Using an Automated High-Altitude Validation Site at Lake Tahoe CA/NV, USA," Geoscience and Remote Sensing, IEEE Transactions on, 43(9), 1991-1999 (2005).
[20] S. J. Hook, R. G. Vaughan, H. Tonooka, and S. G. Schladow, "Absolute Radiometric In-Flight Validation of Mid Infrared and Thermal Infrared Data From ASTER and MODIS on the Terra Spacecraft Using the Lake Tahoe, CA/NV, USA, Automated Validation Site," Geoscience and Remote Sensing, IEEE Transactions on, 45(6), 1798-1807 (2007).
[21] J. A. Barsi, J. R. Schott, S. J. Hook, N. G. Raqueno, B. L. Markham, and R. G. Radocinski, "Landsat-8 Thermal Infrared Sensor (TIRS) Vicarious Radiometric Calibration," Remote Sensing, 6(11), 11607-11626 (2014).
[22] J. S. Czapla-Myers, K. J. Thome, and S. F. Biggar, "Design, calibration, and characterization of a field radiometer using light-emitting diodes as detectors," Applied Optics, 47(36), 6753-62 (2008).
[23] J. S. Czapla-Myers, K. J. Thome, and J. H. Buchanan, "Implication of spatial uniformity on vicarious calibration using automated test sites." Proc. SPIE 6677, 66770U-10 (2007).
[24] J. S. Czapla-Myers, K. J. Thome, B. R. Cocilovo, J. T. McCorkel, and J. H. Buchanan, "Temporal, spectral, and spatial study of the automated vicarious calibration test site at Railroad Valley, Nevada." Proc. SPIE 7081, 70810I-9 (2008).
[25] N. Anderson, J. Czapla-Myers, N. Leisso, S. Biggar, C. Burkhart, R. Kingston, and K. Thome, "Design and calibration of field deployable ground-viewing radiometers," Appl. Opt., 52(2), 231-240 (2013).
[26] N. J. Anderson, and J. S. Czapla-Myers, "Ground viewing radiometer characterization, implementation and calibration applications: a summary after two years of field deployment." Proc. SPIE 8866, 88660N-88660N-10 (2013).
[27] N. Anderson, S. Biggar, K. Thome, and N. Leisso, "Solar radiation-based calibration of laboratory grade radiometers." Proc. SPIE 6677, 66770X-13 (2007).
[28] N. Anderson, K. Thome, J. Czapla-Myers, and S. Biggar, "Design of an ultra-portable field transfer radiometer supporting automated vicarious calibration." Proc. SPIE 9607, 960709-960709-9 (2015).
[29] R. Sumner, "Processing RAW Images in Matlab," Department of Electrical Engineering, University of California Sata Cruz, (2014).